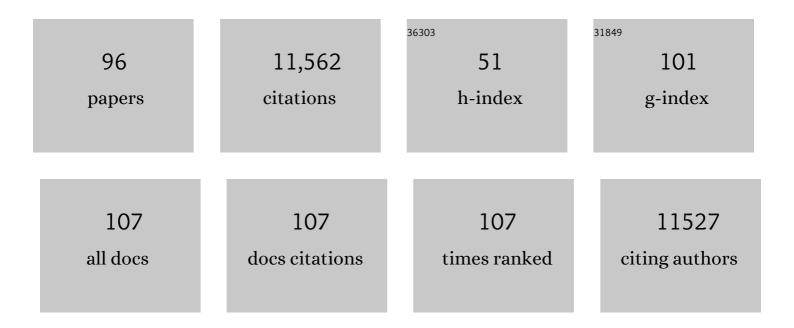
Xianguang Meng

List of Publications by Year in descending order

Source: https://exaly.com/author-pdf/4807224/publications.pdf Version: 2024-02-01



#	Article	IF	CITATIONS
1	Highly efficient solar-driven CO2-to-fuel conversion assisted by CH4 over NiCo-ZIF derived catalysts. Fuel, 2022, 310, 122441.	6.4	9
2	Solarâ€Enhanced CO ₂ Conversion with CH ₄ over Synergetic NiCo Alloy Catalysts with Lightâ€toâ€Fuel Efficiency of 33.8%. Solar Rrl, 2021, 5, 2100185.	5.8	31
3	Au Modified F-TiO2 for Efficient Photocatalytic Synthesis of Hydrogen Peroxide. Molecules, 2021, 26, 3844.	3.8	4
4	Au modified Bi2O3-TiO2 hybrid for photocatalytic synthesis of hydrogen peroxide. Catalysis Communications, 2021, 155, 106315.	3.3	11
5	Insights into the critical dual-effect of acid treatment on ZnxCd1-xS for enhanced photocatalytic production of syngas under visible light. Applied Catalysis B: Environmental, 2021, 288, 119976.	20.2	41
6	Solarâ€Enhanced CO ₂ Conversion with CH ₄ over Synergetic NiCo Alloy Catalysts with Lightâ€ŧoâ€Fuel Efficiency of 33.8%. Solar Rrl, 2021, 5, 2170085.	5.8	3
7	Ca- and Ga-Doped LaMnO ₃ for Solar Thermochemical CO ₂ Splitting with High Fuel Yield and Cycle Stability. ACS Applied Energy Materials, 2021, 4, 9000-9012.	5.1	22
8	Photo-thermal CO2 reduction with methane on group VIII metals: In situ reduced WO3 support for enhanced catalytic activity. Chinese Journal of Catalysis, 2021, 42, 1976-1982.	14.0	20
9	A selective Au-ZnO/TiO2 hybrid photocatalyst for oxidative coupling of methane to ethane with dioxygen. Nature Catalysis, 2021, 4, 1032-1042.	34.4	156
10	A novel "turnâ€on―fluorescent sensor for hydrogen peroxide based on oxidized porous gâ€C 3 N 4 nanosheets. Journal of Biomedical Materials Research - Part B Applied Biomaterials, 2020, 108, 1077-1084.	3.4	4
11	Highly Selective Production of Ethylene by the Electroreduction of Carbon Monoxide. Angewandte Chemie, 2020, 132, 160-166.	2.0	13
12	Highly Selective Production of Ethylene by the Electroreduction of Carbon Monoxide. Angewandte Chemie - International Edition, 2020, 59, 154-160.	13.8	68
13	Au-nanoparticle-supported ZnO as highly efficient photocatalyst for H2O2 production. Catalysis Communications, 2020, 134, 105860.	3.3	39
14	Optimizing Electron Densities of Niâ€N Complexes by Hybrid Coordination for Efficient Electrocatalytic CO ₂ Reduction. ChemSusChem, 2020, 13, 929-937.	6.8	76
15	Frontispiece: Highly Selective Production of Ethylene by the Electroreduction of Carbon Monoxide. Angewandte Chemie - International Edition, 2020, 59, .	13.8	0
16	Frontispiz: Highly Selective Production of Ethylene by the Electroreduction of Carbon Monoxide. Angewandte Chemie, 2020, 132, .	2.0	0
17	Selective Photo-oxidation of Methane to Methanol with Oxygen over Dual-Cocatalyst-Modified Titanium Dioxide. ACS Catalysis, 2020, 10, 14318-14326.	11.2	114
18	A β-cyclodextrin Modified Graphitic Carbon Nitride with Au Co-Catalyst for Efficient Photocatalytic Hydrogen Peroxide Production. Nanomaterials, 2020, 10, 1969.	4.1	15

#	Article	IF	CITATIONS
19	Electrocatalytic Synthesis of Hydrogen Peroxide over Au/TiO ₂ and Electrochemical Trace of OOH* Intermediate. Chemistry - an Asian Journal, 2020, 15, 4280-4285.	3.3	4
20	Distance Synergy of MoS ₂ â€Confined Rhodium Atoms for Highly Efficient Hydrogen Evolution. Angewandte Chemie - International Edition, 2020, 59, 10502-10507.	13.8	122
21	Stabilizing CuGaS ₂ by crystalline CdS through an interfacial Z-scheme charge transfer for enhanced photocatalytic CO ₂ reduction under visible light. Nanoscale, 2020, 12, 8693-8700.	5.6	39
22	Distance Synergy of MoS ₂ â€Confined Rhodium Atoms for Highly Efficient Hydrogen Evolution. Angewandte Chemie, 2020, 132, 10588-10593.	2.0	37
23	Intermolecular cascaded π-conjugation channels for electron delivery powering CO2 photoreduction. Nature Communications, 2020, 11, 1149.	12.8	147
24	Confinement Catalysis with 2D Materials for Energy Conversion. Advanced Materials, 2019, 31, e1901996.	21.0	257
25	Solar-Energy-Mediated Methane Conversion. Joule, 2019, 3, 1606-1636.	24.0	252
26	Acidâ€treated Graphitic Carbon Nitride Nanosheets as Fluorescence Probe for Detection of Hemin. ChemistrySelect, 2019, 4, 8178-8182.	1.5	10
27	Efficient Photocatalytic Hydrogen Peroxide Production over TiO2 Passivated by SnO2. Catalysts, 2019, 9, 623.	3.5	29
28	Hollow Mesoporous Fe2O3 Nanospindles/CNTs Composite: An Efficient Catalyst for High-Performance Li-O2 Batteries. Frontiers in Chemistry, 2019, 7, 511.	3.6	2
29	Direct Methane Conversion under Mild Condition by Thermo-, Electro-, or Photocatalysis. CheM, 2019, 5, 2296-2325.	11.7	331
30	Cation Vacancy-Initiated CO ₂ Photoreduction over ZnS for Efficient Formate Production. ACS Energy Letters, 2019, 4, 1387-1393.	17.4	102
31	Selective light absorber-assisted single nickel atom catalysts for ambient sunlight-driven CO2 methanation. Nature Communications, 2019, 10, 2359.	12.8	185
32	Finely dispersed Au nanoparticles on graphitic carbon nitride as highly active photocatalyst for hydrogen peroxide production. Catalysis Communications, 2019, 123, 69-72.	3.3	63
33	Direct and Selective Photocatalytic Oxidation of CH ₄ to Oxygenates with O ₂ on Cocatalysts/ZnO at Room Temperature in Water. Journal of the American Chemical Society, 2019, 141, 20507-20515.	13.7	253
34	βâ€cyclodextrin modified g ₃ N ₄ nanosheet: a fluorescent drug carrier with ultrahigh drug loading capacity and pHâ€responsive release. Journal of Chemical Technology and Biotechnology, 2019, 94, 628-633.	3.2	36
35	Study on the enhancement of photocatalytic environment purification through ubiquitous-red-clay loading. SN Applied Sciences, 2019, 1, 1.	2.9	4
36	Catalysis with Two-Dimensional Materials Confining Single Atoms: Concept, Design, and Applications. Chemical Reviews, 2019, 119, 1806-1854.	47.7	745

#	Article	IF	CITATIONS
37	Light irradiation enhanced CO2 reduction with methane: A case study in size-dependent optical property of Ni nanoparticles. Catalysis Today, 2019, 335, 187-192.	4.4	29
38	Layered double hydroxides decorated graphic carbon nitride film as efficient photoanodes for photoelectrochemical water splitting. Catalysis Today, 2019, 335, 423-428.	4.4	20
39	Probing the role of nickel dopant in aqueous colloidal ZnS nanocrystals for efficient solar-driven CO2 reduction. Applied Catalysis B: Environmental, 2019, 244, 1013-1020.	20.2	50
40	Unique homo–heterojunction synergistic system consisting of stacked BiOCl nanoplate/Zn–Cr layered double hydroxide nanosheets promoting photocatalytic conversion of CO ₂ into solar fuels. Chemical Communications, 2018, 54, 5126-5129.	4.1	27
41	Efficient photocatalytic CO2 reduction over Co(II) species modified CdS in aqueous solution. Applied Catalysis B: Environmental, 2018, 226, 252-257.	20.2	70
42	Constructing Ordered Threeâ€Ðimensional TiO ₂ Channels for Enhanced Visible‣ight Photocatalytic Performance in CO ₂ Conversion Induced by Au Nanoparticles. Chemistry - an Asian Journal, 2018, 13, 577-583.	3.3	18
43	Light-Enhanced Carbon Dioxide Activation and Conversion by Effective Plasmonic Coupling Effect of Pt and Au Nanoparticles. ACS Applied Materials & amp; Interfaces, 2018, 10, 408-416.	8.0	179
44	Reaction Mechanisms of Wellâ€Defined Metal–N ₄ Sites in Electrocatalytic CO ₂ Reduction. Angewandte Chemie, 2018, 130, 16577-16580.	2.0	44
45	Reaction Mechanisms of Wellâ€Defined Metal–N ₄ Sites in Electrocatalytic CO ₂ Reduction. Angewandte Chemie - International Edition, 2018, 57, 16339-16342.	13.8	328
46	A Promising Application of Optical Hexagonal TaN in Photocatalytic Reactions. Angewandte Chemie - International Edition, 2018, 57, 16781-16784.	13.8	55
47	A Promising Application of Optical Hexagonal TaN in Photocatalytic Reactions. Angewandte Chemie, 2018, 130, 17023-17026.	2.0	7
48	A rapidly room-temperature-synthesized Cd/ZnS:Cu nanocrystal photocatalyst for highly efficient solar-light-powered CO2 reduction. Applied Catalysis B: Environmental, 2018, 237, 68-73.	20.2	65
49	Visible-Light-Mediated Methane Activation for Steam Methane Reforming under Mild Conditions: A Case Study of Rh/TiO ₂ Catalysts. ACS Catalysis, 2018, 8, 7556-7565.	11.2	126
50	Self assembly and controlled drug release of a nano-laminated graphite carbon nitride/methotrexate complex. Journal of Materials Science: Materials in Medicine, 2018, 29, 116.	3.6	8
51	Selective Deposition of Ag ₃ PO ₄ on Specific Facet of BiVO ₄ Nanoplate for Enhanced Photoelectrochemical Performance. Solar Rrl, 2018, 2, 1800102.	5.8	44
52	Efficient photocatalytic CO 2 reduction in all-inorganic aqueous environment: Cooperation between reaction medium and Cd(II) modified colloidal ZnS. Nano Energy, 2017, 34, 524-532.	16.0	74
53	Efficient hydrogen evolution over Sb doped SnO2 photocatalyst sensitized by Eosin Y under visible light irradiation. Nano Energy, 2017, 36, 331-340.	16.0	168
54	Light assisted CO ₂ reduction with methane over SiO ₂ encapsulated Ni nanocatalysts for boosted activity and stability. Journal of Materials Chemistry A, 2017, 5, 10567-10573.	10.3	71

#	Article	IF	CITATIONS
55	Lightâ€5witchable Oxygen Vacancies in Ultrafine Bi ₅ O ₇ Br Nanotubes for Boosting Solarâ€Driven Nitrogen Fixation in Pure Water. Advanced Materials, 2017, 29, 1701774.	21.0	533
56	Elemental Boron for Efficient Carbon Dioxide Reduction under Light Irradiation. Angewandte Chemie, 2017, 129, 5662-5666.	2.0	17
57	Elemental Boron for Efficient Carbon Dioxide Reduction under Light Irradiation. Angewandte Chemie - International Edition, 2017, 56, 5570-5574.	13.8	104
58	Rücktitelbild: Elemental Boron for Efficient Carbon Dioxide Reduction under Light Irradiation (Angew. Chem. 20/2017). Angewandte Chemie, 2017, 129, 5724-5724.	2.0	0
59	Light assisted CO 2 reduction with methane over group VIII metals: Universality of metal localized surface plasmon resonance in reactant activation. Applied Catalysis B: Environmental, 2017, 209, 183-189.	20.2	122
60	Morphology effect of nano-hydroxyapatite as a drug carrier of methotrexate. Journal of Materials Science: Materials in Medicine, 2017, 28, 158.	3.6	14
61	Doping Ba into strontium titanate for enhanced photocatalytic oxygen evolution over its supported Au-based catalysts. Catalysis Communications, 2017, 99, 127-130.	3.3	7
62	Photocatalysis: Lightâ€5witchable Oxygen Vacancies in Ultrafine Bi ₅ O ₇ Br Nanotubes for Boosting Solarâ€Đriven Nitrogen Fixation in Pure Water (Adv. Mater. 31/2017). Advanced Materials, 2017, 29, .	21.0	2
63	Targeting Activation of CO ₂ and H ₂ over Ru‣oaded Ultrathin Layered Double Hydroxides to Achieve Efficient Photothermal CO ₂ Methanation in Flowâ€Type System. Advanced Energy Materials, 2017, 7, 1601657.	19.5	193
64	Hematite homojunctions without foreign element doping for efficient and stable overall water splitting. RSC Advances, 2016, 6, 62263-62269.	3.6	14
65	Promoting Active Species Generation by Plasmon-Induced Hot-Electron Excitation for Efficient Electrocatalytic Oxygen Evolution. Journal of the American Chemical Society, 2016, 138, 9128-9136.	13.7	341
66	Improved Photocatalytic H ₂ Evolution over G arbon Nitride with Enhanced Inâ€Plane Ordering. Small, 2016, 12, 6160-6166.	10.0	48
67	Efficient Visibleâ€Lightâ€Driven Carbon Dioxide Reduction by a Singleâ€Atom Implanted Metal–Organic Framework. Angewandte Chemie - International Edition, 2016, 55, 14310-14314.	13.8	612
68	In Situ Bond Modulation of Graphitic Carbon Nitride to Construct p–n Homojunctions for Enhanced Photocatalytic Hydrogen Production. Advanced Functional Materials, 2016, 26, 6822-6829.	14.9	583
69	Efficient Visible‣ightâ€Ðriven Carbon Dioxide Reduction by a Singleâ€Atom Implanted Metal–Organic Framework. Angewandte Chemie, 2016, 128, 14522-14526.	2.0	174
70	Superfine Ag nanoparticle decorated Zn nanoplates for the active and selective electrocatalytic reduction of CO ₂ to CO. Chemical Communications, 2016, 52, 14105-14108.	4.1	33
71	Nanometals for Solarâ€toâ€Chemical Energy Conversion: From Semiconductorâ€Based Photocatalysis to Plasmonâ€Mediated Photocatalysis and Photoâ€Thermocatalysis. Advanced Materials, 2016, 28, 6781-6803.	21.0	471
72	Surfaceâ€Plasmonâ€Enhanced Photodriven CO ₂ Reduction Catalyzed by Metal–Organicâ€Frameworkâ€Đerived Iron Nanoparticles Encapsulated by Ultrathin Carbon Layers. Advanced Materials, 2016, 28, 3703-3710.	21.0	300

#	Article	IF	CITATIONS
73	Design of PdAu alloy plasmonic nanoparticles for improved catalytic performance in CO2 reduction with visible light irradiation. Nano Energy, 2016, 26, 398-404.	16.0	133
74	Tuning Cu dopant of Zn0.5Cd0.5S nanocrystals enables high-performance photocatalytic H2 evolution from water splitting under visible-light irradiation. Nano Energy, 2016, 26, 405-416.	16.0	78
75	Room-temperature driven and visible light enhanced dehydrogenation reactions catalysed by basic Au/SrTiO ₃ . Journal of Materials Chemistry A, 2016, 4, 1941-1946.	10.3	17
76	Effect of band structure on the hot-electron transfer over Au photosensitized brookite TiO ₂ . Physical Chemistry Chemical Physics, 2016, 18, 3409-3412.	2.8	14
77	Active Sites Implanted Carbon Cages in Core–Shell Architecture: Highly Active and Durable Electrocatalyst for Hydrogen Evolution Reaction. ACS Nano, 2016, 10, 684-694.	14.6	426
78	A Co ₃ O ₄ -embedded porous ZnO rhombic dodecahedron prepared using zeolitic imidazolate frameworks as precursors for CO ₂ photoreduction. Nanoscale, 2016, 8, 6712-6720.	5.6	96
79	Solid-base loaded WO ₃ photocatalyst for decomposition of harmful organics under visible light irradiation. APL Materials, 2015, 3, 104411.	5.1	13
80	Conversion of Carbon Dioxide by Methane Reforming under Visibleâ€Light Irradiation: Surfaceâ€Plasmonâ€Mediated Nonpolar Molecule Activation. Angewandte Chemie - International Edition, 2015, 54, 11545-11549.	13.8	168
81	Natureâ€Inspired Environmental "Phosphorylation―Boosts Photocatalytic H ₂ Production over Carbon Nitride Nanosheets under Visible‣ight Irradiation. Angewandte Chemie - International Edition, 2015, 54, 13561-13565.	13.8	287
82	Exceptional enhancement of H2 production in alkaline environment over plasmonic Au/TiO2 photocatalyst under visible light. APL Materials, 2015, 3, .	5.1	16
83	In situ synthesis of ordered mesoporous Co-doped TiO ₂ and its enhanced photocatalytic activity and selectivity for the reduction of CO ₂ . Journal of Materials Chemistry A, 2015, 3, 9491-9501.	10.3	155
84	A highly durable p-LaFeO ₃ /n-Fe ₂ O ₃ photocell for effective water splitting under visible light. Chemical Communications, 2015, 51, 3630-3633.	4.1	83
85	Crystal-facet-dependent hot-electron transfer in plasmonic-Au/semiconductor heterostructures for efficient solar photocatalysis. Journal of Materials Chemistry C, 2015, 3, 7538-7542.	5.5	55
86	Hematite Films Decorated with Nanostructured Ferric Oxyhydroxide as Photoanodes for Efficient and Stable Photoelectrochemical Water Splitting. Advanced Functional Materials, 2015, 25, 2686-2692.	14.9	223
87	An Amineâ€Functionalized Iron(III) Metal–Organic Framework as Efficient Visibleâ€Light Photocatalyst for Cr(VI) Reduction. Advanced Science, 2015, 2, 1500006.	11.2	364
88	All-solid-state Z-scheme system arrays of Fe ₂ V ₄ O ₁₃ /RGO/CdS for visible light-driving photocatalytic CO ₂ reduction into renewable hydrocarbon fuel. Chemical Communications, 2015, 51, 800-803.	4.1	139
89	Photothermal Conversion of CO ₂ into CH ₄ with H ₂ over Groupâ€VIII Nanocatalysts: An Alternative Approach for Solar Fuel Production. Angewandte Chemie - International Edition, 2014, 53, 11478-11482.	13.8	385
90	Enhancement of photocatalytic activity for WO3 by simple NaOH loading. Applied Catalysis A: General, 2014, 488, 183-188.	4.3	18

#	Article	IF	CITATIONS
91	Nanorod-like α-Bi ₂ O ₃ : a highly active photocatalyst synthesized using g-C ₃ N ₄ as a template. RSC Advances, 2014, 4, 55062-55066.	3.6	22
92	Template-assisted synthesis and novel microwave absorption properties of superparamagnetic 2D-nanolamellar Fe3O4. Materials Research Bulletin, 2014, 49, 176-179.	5.2	11
93	Photocatalytic CO ₂ conversion over alkali modified TiO ₂ without loading noble metal cocatalyst. Chemical Communications, 2014, 50, 11517-11519.	4.1	162
94	Photoreduction of CO 2 over the well-crystallized ordered mesoporous TiO 2 with the confined space effect. Nano Energy, 2014, 9, 50-60.	16.0	137
95	The electrochemical preparation and microwave absorption properties of magnetic carbon fibers coated with Fe3O4 films. Applied Surface Science, 2011, 257, 10808-10814.	6.1	72
96	Synthesis and characterization of a lamellar hydroxyapatite/DNA nanohybrid. Materials Chemistry and Physics, 2011, 126, 470-475.	4.0	36